SRC TR 88-98

TECHNICAL RESEARCH REPORT

Sequential Detection of Unknown Frequency-Hopped Waveforms

by

W. E. Snelling and E. Geraniotis

SYSTEMS RESEARCH CENTER

UNIVERSITY OF MARYLAND

COLLEGE PARK, MARYLAND 20742

SEQUENTIAL DETECTION OF UNKNOWN FREQUENCY-HOPPED WAVEFORMS

William E. Snelling and Evaggelos Geraniotis

Department of Electrical Engineering
and Systems Research Center
University of Maryland
College Park, MD 20742

ABSTRACT

The channelized receiver which is optimal for the detection of unknown non-coherent frequency-hopped waveforms bases its decision on a fixed-length block of input data. In this paper we present a sequential method of interception according to which whenever a new data element is collected, a decision is made as to the presence or non-presence of a frequency-hopped waveform. If that decision was indeterminate, another data element is collected. An optimal sequential test is derived, under the assumption that the waveform signal-to-noise ratio (S/N) is known. It is shown that this sequential test requires less data, on average, than the fixed length method to make a decision with the same reliability.

Also derived is a truncated sequential method where a decision is forced, if still indeterminate, after some set amount of data is collected. The truncated test is shown to improve the number of samples needed for a decision when the input signal-to-noise ratio defers greatly from that assumed in the derivation of the test. Furthermore it is shown, that the truncated test yields a limited degree of robustness when the input S/N defers slightly from that assumed. A detailed analysis of the performance of these tests is conducted from which a method for finding an optimal truncation point follows. Numerical results which are based on this analysis as well as on simulation of the interceptor's performance are presented to prove the claims made above.

This research was supported in part by Contel/Federal Systems Division and in part by the Systems Research Center at the University of Maryland, College Park, through the National Science Foundation's Engineering Research Centers Program: NSF CDR 8803012.

1 Background and Introduction

This paper applies and extents previously published results in sequential detection to the problem of the optimal detection of noncoherent frequency-hopped (FH) waveforms. By using likelihood function methods, the problem was previously solved in [2] for the case of a frequency-hopped waveform with a known signal-to-noise ratio and epochs with known starting times and durations. However, in this approach, the decision was based on a data segment of fixed-size. Here, a sequential approach is taken, meaning that whenever a new data element is collected, a decision is attempted as to the presence or nonpresence of a frequency-hopped waveform. If no decision was reached, another data element is collected.

The sequential approach to detection has a rich history. For the binary hypothesis problem with discrete-time independent identically distributed (i.i.d.) data, Wald [3] has derived the optimal sequential test. This test is optimal in the sense that no other test can reach a decision of the same Neyman-Pearson reliability within a smaller average time. This result has been extended to continuous time data in reference [4] and [5]. Others have suggested tests that must make a decision within a prescribed time. These are the "truncated" tests given in [6], [7], and [8]. Truncation is desirable not only for implementation reasons but to improve the performance of a sequential test when the input statistics differ from those assumed in designing the test. In particular, Tantaratana and Poor in reference [9] derived a truncated sequential test for i.i.d. Gaussian data with an unknown mean. This work is the foundation of the bulk of the results included in this paper.

The process of development of the sequential test is begun by defining the observations model for a composite hypothesis problem. Specifically, given the observation $y(t)$, the problem is one of choosing between H_0, which is the hypothesis that a FH waveform is not present and $H_{\gamma'}$, which is

the hypothesis that a FH waveform is present with a signal-to-noise ratio γ' where $0 < \gamma'$. Exactly, the model is

$$\begin{aligned} H_0: \quad & y(t) = n(t) \\ \text{versus} \qquad & \\ H_{\gamma'}: \quad & y(t) = \sum_{i=1}^{N_h} x_i(t) + n(t) \qquad 0 < \gamma' \end{aligned} \tag{1}$$

where

$x_i(t)$ equals $\sqrt{2S'}\sin(\omega_{k_i}t + \theta_i)$ for $iT_h \leq t \leq (i+1)T_h$.

$n(t)$ is white Gaussian noise with two-sided spectral density $\frac{N_0}{2}$.

ω_{k_i} for $1 \leq k_i \leq K$, is one of a family of known frequencies within the spread spectrum bandwidth with these being uniformly random for each epoch.

θ_i is random phase with uniform distribution.

S' is the average signal energy.

T_h is the epoch, or time duration, of each hop.

N_h is the number of hops over message duration.

The hypothesized signal-to-noise ratio γ' is related to the other model parameters by

$$\gamma' = \frac{S'T_h}{N_0} \tag{2}$$

Because a reliable test cannot be devised for FH waveform with an arbitrarily small signal-to-noise ratio, the preceding composite hypothesis problem is simplified to a binary hypothesis problem: H_0 versus H_γ where γ is specified as the smallest signal-to-noise ratio that is to accurately detected. The quantity γ has value

$$\gamma = \frac{ST_h}{N_0} \tag{3}$$

with S being the corresponding signal energy. Also of use will be a quantity which is identified as the relative signal-to-noise ratio $r = \sqrt{\gamma'/\gamma}$.

Using the above observations model, the design of a sequential test for the detection of FH signals will be approached as follows. An asymptotically optimal test will be derived by applying likelihood function theory to the simplified binary hypothesis problem: H_0 versus H_γ. The parameters of this test will be specified to ensure a maximum probability of detection for a given probability of false alarm. This binary hypothesis test will then be applied to the more general composite hypothesis problem with a resulting degradation for the small signal-to-noise case that will be shown to be partially controllable by properly truncating the test procedure.

The derivation of the asymptotically optimal test will begin with the derivation of the likelihood function for a single-epoch observation which is appropriately called the Single-Epoch Likelihood Function (SELF). Next by invoking the central limit theorem, Gaussian densities will be found that are asymptotic to the actual SELF densities as the number of frequencies becomes large. In determining these densities, the SELF's means and variances will be explicitly computed under each hypothesis. By next considering individual SELFs as the observations, the problem will be reduced to a binary hypothesis problem with Gaussian i.i.d. observations. This simplification will be justified because each epoch of FH waveform has independent statistics and because the SELF's statistics do not depend on the particular hop frequency. Using these equivalent observations and their asymptotic densities, the Asymptotic Log-Likelihood Function (ALLF) will be derived. The ALLF will then be used to synthesize tests for the binary hypothesis problem. This procedure will require extending the previously published sequential tests to the cases of data with variances which depend on the hypothesis. Applying these results, a Fixed-Sample Size (FSS) test, a Sequential Probability Ratio Test (SPRT), and a Truncated Sequential Test (TST) will be designed.

Each of the three tests will be analyzed by approximating the test statistic by a Wiener process

and then employing the classical theory of diffusion as outlined in references [5] and [6]. This analysis will be more general than that used to design the tests in that it will allow the performance of each test to be evaluated for the composite hypothesis problem rather than the assumed binary hypothesis problem. This analysis will yield the average sample time of each test as a function of the input signal-to-noise ratio and will yield the operating characteristic of each test. From these results, a test will be designed that is optimal in the sense that the maximum average sample number with respect to the input signal-to-noise ratio is minimum. Finally, a computer simulation will confirm these analytical results.

To further extend these results to the case of a test that was synthesized under the expectation of detecting a FH waveform with extremely small signal-to-noise ratio, an asymptotic analysis of a different sort will be undertaken. This analysis will show how the above tests perform for the composite hypothesis problem as the minimum reliably detectable signal-to-noise ratio of the FH waveform becomes increasingly small. Numerical results for this case will be given but a corresponding computer simulation is not possible due to the rate of increase of the number of computations required as the signal-to-noise ratio diminishes.

2 Likelihood Function: One Epoch

The statistical test for the composite hypothesis problem is defined by finding an asymptotically optimal test for a binary hypothesis problem and applying that test to the composite case and accepting the resulting degradation. This simplified binary problem consists of the two hypotheses H_0 where no signal is present and H_γ where a signal is present with signal-to-noise ratio γ. For this binary hypothesis problem, Appendix A contains a derivation of the SELF which is the likelihood

function Λ_i of the ith-epoch observation $y(t)$ for $iT_h < t \leq (i+1)T_h$. The SELF is expressed as

$$\Lambda_i(y) \triangleq E_k\left[\Lambda_i(y/k)\right] \tag{4}$$

$$= \frac{e^{-\gamma}}{K}\sum_{k=0}^{K-1} I_0\left(\sqrt{2\gamma}\sqrt{P_k^2+Q_k^2}\right) \tag{5}$$

where I_0 is the zeroth order modified Bessel function of the first kind and

$$\begin{aligned} P_k &= \frac{2}{\sqrt{N_0 T_h}}\int_{iT_h}^{(i+1)T_h} y(t)\cos\omega_{k_i} t\, dt \\ Q_k &= \frac{2}{\sqrt{N_0 T_h}}\int_{iT_h}^{(i+1)T_h} y(t)\sin\omega_{k_i} t\, dt \end{aligned} \tag{6}$$

Because of the statistical independence between their respective observations, the likelihood function of the n-epoch observation is then $\prod_{i=1}^{n}\Lambda_i$, i.e. , the product of these individual single-epoch likelihood functions.

The SELF is nicely interpreted as the configuration of well-known devices as indicated in Figure 1. That is, the SELF is channelized where each channel has a matched filter that is tuned to a particular hop frequency and whose output is envelope-detected and emphasized by a Bessel function non-linearity. The output of each channel, after scaling by $e^{-\gamma}/K$, is summed to produce the SELF.

3 Asymptotic Log-Likelihood Function

The Asymptotic Log-likelihood Function (ALLF) is asymptotic to the n-epoch likelihood function, $\prod_{i=1}^{n}\Lambda_i$), as the number of FH channels becomes large. The critical idea behind the derivation of the ALLF is the application of the central limit theorem to yield asymptotic densities for the SELF from which, using an n-epoch collection of SELF's as an equivalent observation set, the ALLF will be determined.

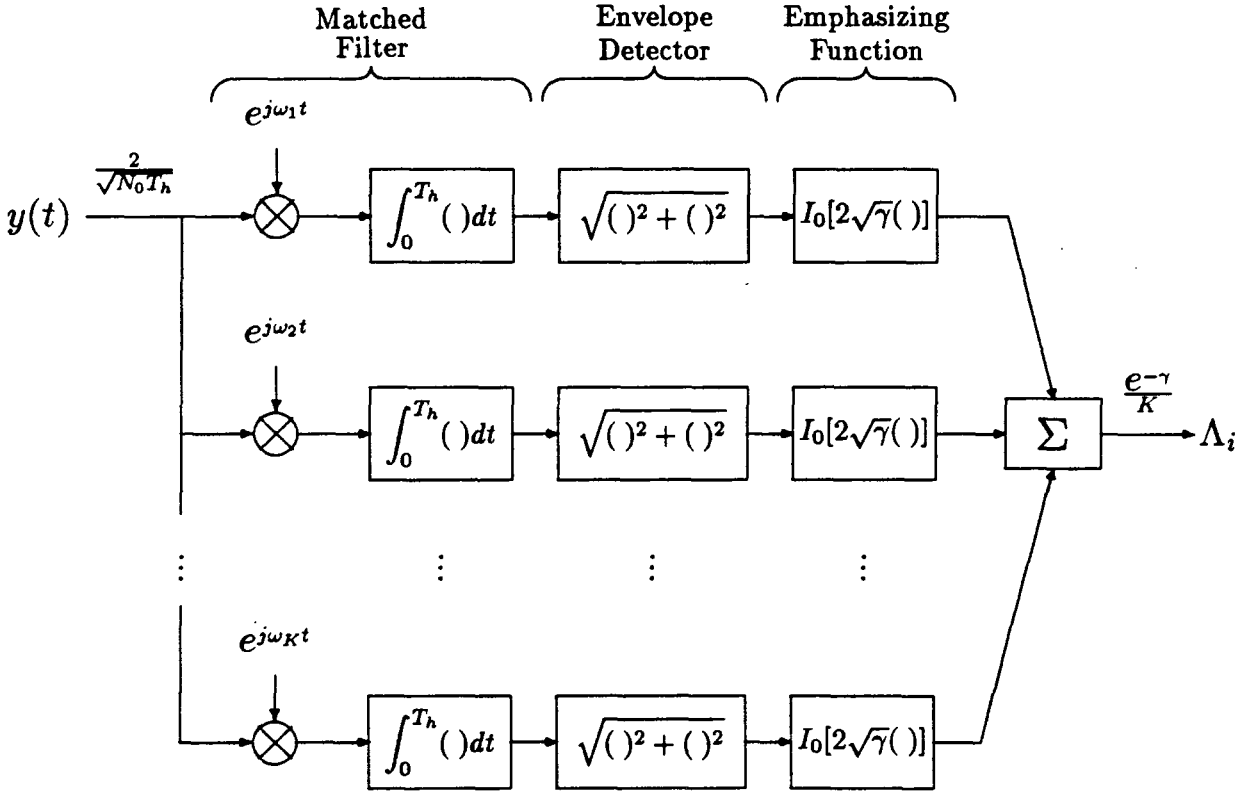

Figure 1: Block Diagram of Single-Epoch Likelihood Function

The SELF (5) was computed assuming a binary hypothesis problem, i.e. , H_0 is the hypothesis that no FH waveform is present, while, H_γ is the hypothesis that a FH waveform exists of a known signal-to-noise ratio γ. The following analysis will assume that a FH waveform, if present, will have a signal-to-noise ratio γ' or equivalently an average signal energy S' that is not necessarily equal to the average signal energy S assumed known in the binary case. This generalization is not necessary to derive the ALLF but will be needed to analyze the performance of the ALLF in the composite hypothesis problem.

Proceeding with the derivation of the ALLF, the central limit theorem is to applied to the SELF to obtain an asymptotic density under all hypothesis's, $0 \leq \gamma'$. The central limit theorem is justified here because the SELF's output is the sum of many channels whose statistics will be shown to be nearly independent and nearly identical. The central limit theorem requires only the mean and variance of each channel and thus only the statistics of the matched filter outputs need be determined exactly since the SELF's mean and variances can be determined from these moments alone.

3.1 Matched Filter Output Statistics

To determine the matched filter output statistics, assume the signal present is in the kth channel then the match filter output in the lth channel can be found from (6) as

$$P_l = \frac{2\sqrt{2\gamma'}}{T_h} \int_{iT_h}^{(i+1)T_h} \sin(\omega_k t + \theta) \cos \omega_l t \, dt + \nu_l \tag{7}$$

$$Q_l = \frac{2\sqrt{2\gamma'}}{T_h} \int_{iT_h}^{(i+1)T_h} \sin(\omega_k t + \theta) \sin \omega_l t \, dt + \xi_l \tag{8}$$

where

$$\begin{aligned} \nu_l &\triangleq \frac{2}{\sqrt{N_0 T_h}} \int_{iT_h}^{(i+1)T_h} n(t) \cos \omega_l t \, dt \\ \xi_l &\triangleq \frac{2}{\sqrt{N_0 T_h}} \int_{iT_h}^{(i+1)T_h} n(t) \sin \omega_l t \, dt \end{aligned} \tag{9}$$

By applying a trigonometric identity, the first components of the matched filter outputs are rewritten as

$$P_l = \delta + \epsilon + \nu_l \tag{10}$$

where

$$\delta = \frac{\sqrt{2\gamma'}}{T_h} \int_{iT_h}^{(i+1)T_h} \sin(\omega_k - \omega_l)t \, dt \tag{11}$$

$$\epsilon = \frac{\sqrt{2\gamma'}}{T_h} \int_{iT_h}^{(i+1)T_h} \sin[(\omega_k + \omega_l)t + 2\theta \,] dt \tag{12}$$

But assuming the channel frequencies are orthogonally spaced, i.e. $(\omega_k - \omega_l)T_h/2\pi$ is an integer and applying the inequality

$$|\epsilon| \leq \frac{2\sqrt{2\gamma'}}{(\omega_k + \omega_l)T_h} \tag{13}$$

we have

$$P_l \approx \begin{cases} \sqrt{2\gamma'} \sin\theta + \nu_l & \text{for } l = k \\ \nu_l & \text{for } l \neq k \end{cases} \tag{14}$$

whenever

$$(\omega_k + \omega_l)T_h \gg 2\sqrt{2\gamma'} \qquad \text{for all } l, k \tag{15}$$

By similar reasoning, and under the same assumptions, the second component of the matched filter output is

$$Q_l \approx \begin{cases} \sqrt{2\gamma'} \cos\theta + \xi_l & \text{for } l = k \\ \xi_l & \text{for } l \neq k \end{cases} \tag{16}$$

The two assumptions made in determining these approximate expressions for the matched filter outputs can be described below. The first assumption is that $\omega_k T_h$ is large and is equivalent to requiring a large number of carrier cycles over a single epoch. The second assumption of orthogonally spaced channels [i.e. $(\omega_k - \omega_l)T_h/2\pi$ is an integer] means, in essence, that the channels are isolated from one another. Another condition implying channel isolation is wide spacing between the channels (i.e. $(\omega_k - \omega_l)T_h$ is large). In a practical implementation, smooth window functions could also have been used in the matched filter implementation to achieve the channel isolation assumed here. The matched filter outputs for no signal present hypothesis H_0 are the special case of the above expressions for $\gamma' = 0$ except they are exact, i.e. ,

$$\begin{aligned} P_l &= \nu_l \\ Q_l &= \xi_l \end{aligned} \tag{17}$$

Simplified expressions for the match filter outputs, (14), (16), and (17) have been derived. The statistical nature of their noise components, $\{\nu_l\}$ and $\{\xi_l\}$, will be determined next. From (9), it follows that the random variables $\{\nu_l\}, \{\xi_l\}$ are Gaussian with zero mean and unity variance. Under the isolated channel assumption, it is easy to show that

$$\begin{aligned} E[\nu_m \nu_n] &= 0 \quad \text{for } m \neq n \quad 1 \leq m, n \leq K \\ E[\nu_m \xi_n] &= 0 \quad \text{for all } m, n \quad 1 \leq m, n \leq K \\ E[\xi_m \xi_n] &= 0 \quad \text{for } m \neq n \quad 1 \leq m, n \leq K \end{aligned} \tag{18}$$

Thus $\{\nu_l\}, \{\xi_l\}$ are mutually independent, since they are Gaussian. These relations also determine the joint density of ν_l and ξ_l as

$$p_{\nu_l, \xi_l}(\nu_l, \xi_l) = \frac{1}{2\pi} e^{-\frac{1}{2}(\nu_l^2 + \xi_l^2)} \tag{19}$$

The equations (14), (16), (17), and (18) along with the joint density of ν_l and ξ_l (19), constitute a complete statistical description of the matched filter outputs $\{P_l\}$ and $\{Q_l\}$.

3.2 SELF Moments

The statistics of $\{P_l\} and \{Q_l\}$ were found in order to determine the mean and variance of the SELF (5). The SELF moments are needed to apply the central limit theorem and thus ultimately produce the ALLF. A few conditions for the application of the central limit theorem will be established now. First, since the random variables $\{P_l\}$ and $\{Q_l\}$ are mutually independent, each channel output of the SELF is also independent. Furthermore, the channel outputs are all identically distributed except for the output of the channel with the signal present. This deviant channel output will be shown to have a variance comparable to that of the other channel outputs and thus, the central limit theorem still applies and with it, we get an density asymptotic to the actual SELF density.

To continue, we need explicit expressions for the mean and variance of the SELF. Assuming a signal is present with a relative signal-to-noise ratio of $r = \sqrt{\gamma'/\gamma}$, then the matched filter outputs of the channel containing the signal are by (14) and (16)

$$\begin{aligned} P_l &= \sqrt{2\gamma'}\sin\theta + \nu_l \\ Q_l &= \sqrt{2\gamma'}\cos\theta + \xi_l \end{aligned} \tag{20}$$

If μ_r and σ_r^2 are defined to be the mean and variance for this channel output, then (19) implies

$$\mu_r = E\left[I_0\left(\sqrt{2\gamma}\sqrt{P_l^2 + Q_l^2}\right)\right] \tag{21}$$

$$= \frac{1}{2\pi}\int_{-\infty}^{\infty}\int_{-\infty}^{\infty} I_0\left(\sqrt{2\gamma}\sqrt{P_l^2 + Q_l^2}\right)e^{-\frac{1}{2}(\nu_l^2+\xi_l^2)}d\nu_l d\xi_l \tag{22}$$

With the rectangular-to-polar conversion, $P_l = \rho\cos\theta$, $Q_l = \rho\sin\theta$, and applying the identity

$$I_0(a) = \frac{1}{2\pi}\int_0^{2\pi} e^{a\cos\theta}d\theta \tag{23}$$

the integral becomes

$$\mu_r = e^{-\gamma} \int_0^\infty \rho I_0\left(\sqrt{2\gamma}\rho\right) I_0\left(\sqrt{2\gamma'}\rho\right) e^{-\frac{\rho^2}{2}} d\rho \tag{24}$$

$$= e^{\gamma} I_0(2\sqrt{\gamma\gamma'}) \tag{25}$$

This integral was evaluated in [10], §13.31(1). The variance is now evaluated as follows

$$\sigma_r^2 + \mu_r^2 = E\left[I_0^2\left(\sqrt{2\gamma}\sqrt{P_l^2 + Q_l^2}\right)\right] \tag{26}$$

$$= \frac{1}{4\pi} \int_{-\infty}^{\infty} \int_{-\infty}^{\infty} I_0^2\left(\sqrt{2\gamma}\sqrt{P_l^2 + Q_l^2}\right) e^{-\frac{1}{2}(\nu_l^2 + \xi_l^2)} d\nu_l d\xi_l \tag{27}$$

which becomes with rectangular-to-polar conversion, and applying (23)

$$\sigma_r^2 + \mu_r^2 = e^{-\gamma} \int_0^\infty \rho I_0^2\left(\sqrt{2\gamma}\rho\right) I_0\left(\sqrt{2\gamma'}\rho\right) e^{-\frac{\rho^2}{2}} d\rho \tag{28}$$

This integral is evaluated by applying a formula from [10], §11.41(16) which states

$$\frac{1}{\pi} \int_0^\pi J_0(a^2 + b^2 - 2ab\cos\theta) d\theta = I_0(a) I_0(b) \tag{29}$$

where J_0 is the zeroth-order Bessel function. Application of this formula and an interchange of integrations reduces the integral (28) to a simpler integral solved in [10], §13.31(1). The net result is

$$\sigma_r^2 + \mu_r^2 = \frac{e^{2\gamma}}{\pi} \int_0^\pi e^{-2\gamma\cos\phi} I_0(4\sqrt{\gamma\gamma'}\sin\tfrac{\phi}{2}) d\phi \tag{30}$$

Summarizing, for a signal in channel l with signal-to-noise γ', the channel moments are

$$\begin{aligned} \mu_r &= e^{\gamma} I_0(2r\gamma) \\ \sigma_r^2 &= e^{2\gamma}\left[\frac{1}{\pi}\int_0^\pi e^{-2\gamma\cos\phi} I_0\left(4r\gamma\sin\tfrac{\phi}{2}\right) d\phi - I_0^2(2r\gamma)\right] \end{aligned} \tag{31}$$

where $r = \sqrt{\gamma'/\gamma}$.

The above calculations give expressions for the channel moments for a channel with a signal present. The moments for the case of a channel without a signal present are special cases of the above with $r = 0$ and are thus denoted μ_0 and σ_0^2. From (31) and the Bessel function identity (23), they are

$$\begin{aligned} \mu_0 &= e^{\gamma} \\ \sigma_0^2 &= e^{2\gamma}[I_0(2\gamma) - 1] \end{aligned} \tag{32}$$

Likewise, moments for channel l containing a signal of the maximum strength γ correspond to $r = 1$ and are thus denoted μ_1 and σ_1^2.

Expressions for the mean and variance of the SELF are now immediate since the SELF is the sum of all K channels scaled by $e^{-\gamma}/K$. The expressions are

$$M_0 = e^{-\gamma}\mu_0 \tag{33}$$

$$V_0 = \frac{e^{-2\gamma}}{K}\sigma_0^2 \tag{34}$$

$$M_r = \frac{e^{-\gamma}}{K}[(K-1)\mu_0 + \mu_r] \tag{35}$$

$$V_r = \frac{e^{-2\gamma}}{K^2}\left[(K-1)\sigma_0^2 + \sigma_r^2\right] \tag{36}$$

$$M_1 = \frac{e^{-\gamma}}{K}[(K-1)\mu_0 + \mu_1] \tag{37}$$

$$V_1 = \frac{e^{-2\gamma}}{K^2}\left[(K-1)\sigma_0^2 + \sigma_1^2\right] \tag{38}$$

where M_r is the mean of the SELF when a signal of strength γ' is present while M_0 and M_1 are special cases of M_r when $r = 0$ and $r = 1$, respectively. The variances, V_r, V_0, and V_1 are defined similarly.

3.3 Derivation of the ALLF

With the first two moments of the SELF determined, the central limit theorem gives approximating densities to the SELF, Λ_i, under the composite hypothesis problem. These densities are

$$\begin{array}{lll} & H_0: \quad \Lambda_i \sim \frac{1}{\sqrt{2\pi V_0}} e^{-\frac{(\Lambda_i - M_0)^2}{2V_0}} & \\ \text{versus} & & \\ & H_{\gamma'}: \quad \Lambda_i \sim \frac{1}{\sqrt{2\pi V_r}} e^{-\frac{(\Lambda_i - M_r)^2}{2V_r}} & \text{for } 0 < \gamma' \leq \gamma \end{array} \tag{39}$$

which gives a simplified statistical characterization of the SELF. That is, the SELF outputs, $\{\Lambda_i\}$, are Gaussian i.i.d. variables whose means and variance depend on the hypothesis.

As was the procedure in deriving the SELF, the asymptotic log-likelihood function (ALLF) will be designed using the simpler binary hypothesis problem. For a single-epoch, likelihood ratio theory and (39) implies a log-likelihood ratio of

$$L_i(\Lambda_i) = c_2 \Lambda_i^2 + c_1 \Lambda_i + c_0 \tag{40}$$

where

$$c_2 = \frac{1}{2}\left(\frac{1}{V_0} - \frac{1}{V_1}\right) \tag{41}$$

$$c_1 = \left(\frac{M_1}{V_1} - \frac{M_0}{V_0}\right) \tag{42}$$

$$c_0 = \frac{1}{2}\left(\frac{M_0^2}{V_0} - \frac{M_1^2}{V_1} + \ln\frac{V_0}{V_1}\right) \tag{43}$$

Independence between observations over different epochs, implies that the ALLF up to time n is,

$$T_n = \sum_{i=1}^{n} L_i \tag{44}$$

And the ALLF has now been found.

3.4 Moments of the ALLF

For the analysis to follow, it will prove useful to derive the moments of L_i from which the ALLF moments follow trivially from (44). Starting with the mean,

$$\mathcal{M}_r \triangleq E\left[L_i\left(\Lambda_i\right)\right] \tag{45}$$

$$= c_2 E(\Lambda_i^2) + c_1 E(\Lambda_i) + c_0 \tag{46}$$

$$= c_2\left(M_r^2 + V_r\right) + c_1 M_r + c_0 \tag{47}$$

which expands in terms of the SELF moments to

$$\mathcal{M}_r = \frac{1}{2}\ln\frac{V_0}{V_1} + (2V_1V_0)^{-1}\left[(M_r - M_0)^2 V_1 + (M_r - M_1)^2 V_0 + (V_1 - V_0)V_r\right] \tag{48}$$

Now to compute the variance of L_i.

$$\mathcal{V}_r = Var\left[L_i\left(\Lambda_i\right)\right] \tag{49}$$

which upon substitution of (40) yields,

$$\mathcal{V}_r = Var\left[c_2\Lambda_i^2 + c_1\Lambda_i + c_0\right] \tag{50}$$

$$= Var\left[(c_2M_r^2 + c_1M_r + c_0) + (2c_2M_r + c_1)v + c_2v^2\right] \tag{51}$$

where $v = \Lambda_i - M_r$ Proceeding,

$$\mathcal{V}_r = Var\left[(2c_2M_r + c_1)\,v + c_2v^2\right] \tag{52}$$

$$= (2c_2M_r + c_1)^2 V_r + 2c_2^2V_r^2 \tag{53}$$

which simplifies to

$$\mathcal{V}_r = \frac{V_r^2}{2}\left(\frac{1}{V_0} - \frac{1}{V_1}\right)^2 + \left[\left(\frac{1}{V_0} - \frac{1}{V_1}\right)M_r + \left(\frac{M_1}{V_1} - \frac{M_0}{V_0}\right)\right]^2 V_r \tag{54}$$

The special cases, $r = 1$ and $r = 0$, of the moments of L_i are included here for convenience. They are

$$\mathcal{M}_0 = \frac{1}{2}\ln\frac{V_0}{V_1} + \frac{1}{2V_1}\left[V_1 - V_0 - (M_1 - M_0)^2 + V_1\right] \tag{55}$$

$$\mathcal{M}_1 = \frac{1}{2}\ln\frac{V_0}{V_1} + \frac{1}{2V_0}\left[V_1 - V_0 + (M_1 - M_0)^2 + V_0\right] \tag{56}$$

$$\mathcal{V}_0 = \frac{1}{2}\left(\frac{V_0}{V_1} - 1\right)^2 + \frac{V_0}{V_1^2}(M_1 - M_0)^2 \tag{57}$$

$$\mathcal{V}_1 = \frac{1}{2}\left(\frac{V_1}{V_0} - 1\right)^2 + \frac{V_1}{V_0^2}(M_1 - M_0)^2 \tag{58}$$

3.5 Summary

A log-likelihood function for the binary hypothesis problem, designated the ALLF, has been derived that is asymptotic to the true log-likelihood function as the number of channels becomes large. The ALLF was found with likelihood ratio theory by considering an n-epoch collection of SELFs as a set of i.i.d. observations, assumed Gaussian by the central limit theorem. The Gaussian assumption was justified by showing that each SELF was the sum of nearly independent and nearly identical random variables. Also derived were various means and variances that will prove useful in future discussions. The ALLF will now be used to design a FSS test, SPRT, and a TST.

4 Test Design

The results above reduced the problem of detecting a FH waveform to that of discriminating between two sets of Gaussian i.i.d. data with different means and variances. A Fixed Sample Size (FSS) test, a Sequential Probability Ratio Test (SPRT), and a Truncated Sequential Test (TST) based on this simplified model will be discussed.

4.1 FSS Test Design

As the name suggests, a FSS test consists of comparing a test statistic T_L, based on a fixed number L of observations, to a threshold τ. Then if the test statistic is greater than τ, the hypothesis H_1 is chosen while correspondingly a test statistic less than τ indicates hypothesis H_0. Symbolically this is,

$$T_L \begin{cases} \geq \tau & \Rightarrow \quad H_1 \\ < \tau & \Rightarrow \quad H_0 \end{cases} \tag{59}$$

In our case, the test statistic is the L-epoch ALLF and the test parameters, L and τ, are specified to correspond to prescribed false alarm P_F and detection P_D probabilities. To determine L and τ, the density of the T_L is needed for each hypothesis. Although this density equals the non-central χ^2 density, an approximate Gaussian density, derived via the central limit theorem, is used instead to yield simplified expressions for the test parameters. From these densities, P_D and P_F can be computed in terms of L and τ and solved to yield,

$$L = \frac{\left[\mathcal{V}_1^{\frac{1}{2}}\Phi^{-1}(1-P_D) - \mathcal{V}_0^{\frac{1}{2}}\Phi^{-1}(1-P_F)\right]^2}{(\mathcal{M}_1 - \mathcal{M}_0)^2} \tag{60}$$

$$\tau = \frac{L^{\frac{1}{2}}}{(\mathcal{M}_1 - \mathcal{M}_0)}\left[\mathcal{V}_0^{\frac{1}{2}}\mathcal{M}_1\Phi^{-1}(1-P_F) - \mathcal{V}_1^{\frac{1}{2}}\mathcal{M}_0\Phi^{-1}(1-P_D)\right] \tag{61}$$

4.2 SPRT Design

Wald's sequential probability ratio test (SPRT) can now be defined as a test with test statistic T_n, based on n observations and two thresholds, a and b. The SPRT works as follows. Upon the nth observation, if T_n is greater than a, then the hypothesis H_1 is chosen. If T_n is less than b, then

the hypothesis H_0 is chosen. If, instead, T_n is between a and b, the test statistic is updated to include $n+1$ observations and the process is iterated. Symbolically this test is described as

$$\text{for each } n,\ T_n \begin{cases} \geq a & \Rightarrow \quad H_1 \\ \leq b & \Rightarrow \quad H_0 \\ \in (a,b) & \Rightarrow \quad \text{take another sample} \end{cases} \tag{62}$$

The threshold values, a and b, are assigned to give the desired Neyman-Pearson probabilities; probability of detection P_D and probability of false alarm P_F. Relationships between the thresholds and the Neyman-Pearson probabilities are given by Wald's approximations [3],

$$a \approx \ln\left(\frac{1-P_D}{1-P_F}\right) \tag{63}$$

$$b \approx \ln\left(\frac{P_D}{P_F}\right) \tag{64}$$

which completes the specification of Wald's SPRT.

4.3 TST Design

TST is a hybrid of the above two tests. Specifically, TST follows the rules of a sequential test with test statistic T_n and with thresholds, a and b, but has the added feature of forcing a decision at time L (if no decision has yet been made) by comparing the test statistic to a threshold τ. Symbolically,

$$\begin{aligned} &\text{for each } n < L,\ T_n \begin{cases} \geq a & \Rightarrow \quad H_1 \\ \leq b & \Rightarrow \quad H_0 \\ \in (a,b) & \Rightarrow \quad \text{take another sample} \end{cases} \\ &\text{but for } n = L,\quad T_L \begin{cases} \geq \tau & \Rightarrow \quad H_1 \\ < \tau & \Rightarrow \quad H_0 \end{cases} \end{aligned} \tag{65}$$

Two relations secure the specification of the TST parameters, a, b, L, and τ. If P_F^* and P_D^* are the actual Neyman-Pearson probabilities for the TST, then from [7]

$$P_F^* \leq P_F^{FSS} + P_F^{SPRT} \tag{66}$$

$$(1 - P_D^*) \leq (1 - P_D^{FSS}) + (1 - P_D^{SPRT}) \tag{67}$$

where P_F^{FSS} is the probability of false-alarm for the TST if $L = \infty$ and P_F^{SPRT} is the false-alarm probability for the TST if $a = -b = \infty$. P_D^{FSS} and P_D^{SPRT} are defined similarly. Thus, the errors of the TST can be viewed as a mixture of the errors of a FSS test with parameters, L and τ and a SPRT with parameters, a and b. These inequalities can be verified by viewing the ALLF, T_n, as a discrete stochastic process with time index n, and enumerating it's sample paths. For instance, a sample path leading to a false alarm must either cross threshold a before threshold b and before time L or be greater than threshold τ at time L. Since these events also correspond to false alarms in either the FSS test part or the SPRT part of the TST, the inequality (66) must follow.

The above inequalities can be used to specify a TST whose actual error probabilities, P_F^* and $1 - P_D^*$, are less than any specified error probabilities, P_F and $1 - P_D$. Thus, the TST can be designed by partitioning the bounding errors, $(1 - P_D)$ and P_F among the SPRT and FSS test parts of the TST and then using the appropriate parameter equation, given above, to compute the parameters; L, τ, a, and b for TST [7]. Specifically, this partitioning is quantified with the introduction of two constants, $0 \leq C_1 \leq 1$ and $0 \leq C_2 \leq 1$, which are defined as TST mixture constants, the following can be constructed

$$P_F^{FSS} = C_1 P_F \tag{68}$$

$$P_F^{SPRT} = (1 - C_1) P_F \tag{69}$$

$$(1 - P_D^{FSS}) = C_2 (1 - P_D) \tag{70}$$

$$(1 - P_D^{SPRT}) = (1 - C_2)(1 - P_D) \tag{71}$$

for the error probabilities of the FSS test and SPRT parts of the TST. From the above inequalities

and (60), (61), (63), and (64), the TST parameters are determined as follows

$$L = \frac{\left[\mathcal{V}_1^{\frac{1}{2}}\Phi^{-1}(1-P_D^{FSS}) - \mathcal{V}_0^{\frac{1}{2}}\Phi^{-1}(1-P_F^{FSS})\right]^2}{(\mathcal{M}_1-\mathcal{M}_0)^2} \tag{72}$$

$$\tau = \frac{L^{\frac{1}{2}}}{(\mathcal{M}_1-\mathcal{M}_0)}\left[\mathcal{V}_0^{\frac{1}{2}}\mathcal{M}_1\Phi^{-1}(1-P_F^{FSS}) - \mathcal{V}_1^{\frac{1}{2}}\mathcal{M}_0\Phi^{-1}(1-P_D^{FSS})\right] \tag{73}$$

$$a = \ln\left(\frac{1-P_D^{SPRT}}{1-P_F^{SPRT}}\right) \tag{74}$$

$$b = \ln\left(\frac{P_D^{SPRT}}{P_F^{SPRT}}\right) \tag{75}$$

Note that (66) and (67) guarantee that the actual detection errors;

$$P_F^* \leq P_F \tag{76}$$

$$1-P_D^* \leq 1-P_D \tag{77}$$

The mixture constants, C_1 and C_2, reflect proportions of the FSS test and SPRT parts of the TST since if $C_1 = C_2 = 1$, a pure FSS test is defined and if $C_1 = C_2 = 0$, a pure SPRT is defined. Criteria for choosing the mixture constants will be discussed in Section 6.

5 Performance of Tests

The preceding tests, the FSS test, the SPRT, and the TST were designed under the assumption of binary hypotheses. These hypotheses are H_0, FH waveform is not present, and H_γ, FH waveform is present and has signal-to-noise ratio γ. Of concern here is the performance of the three tests when the actual signal-to-noise ratio γ' of the FH waveform is more generally $0 < \gamma' \leq \gamma$. Two parameters characterize a test's performance for a particular γ'. The first, denoted by $E(N/\gamma')$, is the Average Sample Number (ASN) which is defined as the average of the number of samples

needed to reach a decision. The second parameter, denoted $P_0(\gamma')$, is the Operating Characteristic (OC) which is defined as the probability of declaring the absence of a FH waveform for a given γ'.

5.1 Analysis

For the FSS test, the ASN is obviously L, while the OC can be determined by approximating the ALLF at time L by a Gaussian random variable with the same moments. This central-limit-theorem argument produces

$$P_0(\gamma') = \Phi\left(\frac{\tau - L\mathcal{M}_r}{\sqrt{L\mathcal{V}_r}}\right) \tag{78}$$

for the OC.

For the sequential test, the analysis is harder but can be approached as a diffusion problem. Here, we approximate the test statistic by a Wiener process. Specifically, if $T(t)$ is a Wiener process with variance function $\mathcal{V}_r t$ and mean function $\mathcal{M}_r t$, then the ALLF, T_n, converges weakly to $T(t)$ at integer times $t = n$ provided n is sufficiently large. This last restriction is needed to ensure that T_n has approximately a Gaussian density as implied by the central limit theorem. In terms of the approximating Wiener process $T(t)$, the problem of finding the OC function is now the problem of finding the probability that $T(t)$ will "touch" the lower threshold b before the upper threshold a. Likewise, the problem of finding the ASN is now the problem of finding the average time that $T(t)$ first "touches" either threshold,(a or b). This time is also called the average stopping time. Expressions for these quantities are given in [5] and [6] as

$$P_0(\gamma') = \begin{cases} \dfrac{e^{-2b\frac{\mathcal{M}_r}{\mathcal{V}_r}} - 1}{e^{-2b\frac{\mathcal{M}_r}{\mathcal{V}_r}} - e^{-2a\frac{\mathcal{M}_r}{\mathcal{V}_r}}} & \mathcal{M}_r \neq 0 \\ \dfrac{a}{a-b} & \mathcal{M}_r = 0 \end{cases} \tag{79}$$

$$E(N/\gamma') = \begin{cases} \dfrac{aP(\gamma') + b(1 - P(\gamma')}{\mathcal{M}_r} & \mathcal{M}_r \neq 0 \\ -\dfrac{ab}{\mathcal{V}_r} & \mathcal{M}_r = 0 \end{cases} \tag{80}$$

The diffusion technique also applies to the TST, albeit more involved. The ASN is by [5],

$$E(N/\gamma') = A \sum_{n=1}^{\infty} (-1)^n \frac{n}{k_n^2} B_n (e^{-k_n L} - 1) \tag{81}$$

where

$$A = \frac{\mathcal{V}_r \pi}{(a-b)^2} \tag{82}$$

$$B_n = e^{\frac{\mathcal{M}_r b}{\mathcal{V}_r}} \sin \frac{n\pi a}{a-b} - e^{\frac{\mathcal{M}_r a}{\mathcal{V}_r}} \sin \frac{n\pi b}{a-b} \tag{83}$$

$$k_n = \frac{\mathcal{M}_r^2}{2\mathcal{V}_r} + \frac{\mathcal{V}_r n^2 \pi^2}{2(a-b)^2} \tag{84}$$

The OC function defined is by [6],

$$\begin{aligned} P_0(\gamma') = {} & \Phi\left(\frac{\tau - L\mathcal{M}_r}{\sqrt{L\mathcal{V}_r}}\right) \\ & - \sum_{r=1}^{\infty} e^{2\frac{\mathcal{M}_r}{\mathcal{V}_r}[na-(n-1)b]} \Phi\left(\frac{\tau - L\mathcal{M}_r - 2[na-(n-1)b]}{\sqrt{L\mathcal{V}_r}}\right) \\ & + e^{2\frac{\mathcal{M}_r}{\mathcal{V}_r} n(a-b)} \Phi\left(\frac{\tau - L\mathcal{M}_r - 2n(a-b)}{\sqrt{L\mathcal{V}_r}}\right) \\ & + e^{2\frac{\mathcal{M}_r}{\mathcal{V}_r}[nb-(n-1)a]} \Phi\left(\frac{2[nb-(n-1)a] - \tau + L\mathcal{M}_r}{\sqrt{L\mathcal{V}_r}}\right) \\ & - e^{2\frac{\mathcal{M}_r}{\mathcal{V}_r} n(b-a)} \Phi\left(\frac{2n(b-a) - \tau + L\mathcal{M}_r}{\sqrt{L\mathcal{V}_r}}\right) \end{aligned} \tag{85}$$

These equations represent a complete characterization of the FSS test, SPRT, and TST.

The fact that the diffusion technique yields accurate expressions for the ASN and OC functions will not be proved here but will be verified below by a computer simulation.

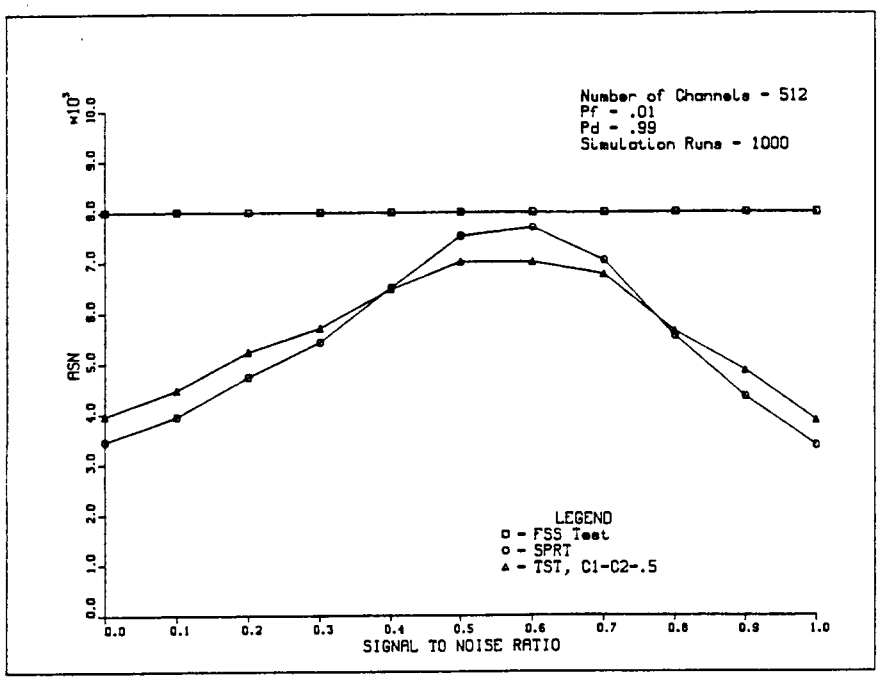

Figure 2: ASN from Simulation versus S/N, $\gamma = 1$

5.2 Numerical Results

The FSS test, SPRT, and TST were simulated, by computer, to prove the assumptions of the analysis and as an independent measure of the relative performance of the three tests. The simulated detector consists of 512 channels and each test was synthesized to ensure a probability of false alarm P_f of no more than 1% and a probability of detection P_D of at least 99 %. Under these specifications, the detector was simulated until 1000 decisions were reached for each of 11 signal-to-noise ratios evenly spaced between 0 and γ. The decisions that no FH waveform was present were averaged to estimate the OC, while the number of observations taken to reach a decision were averaged to estimate the ASN. Additionally, the standard deviation of ASN average was measured to indicate the ASN estimation error.

Figure 2 and Figure 3 are, respectively, the ASNs by simulation and by theory when the

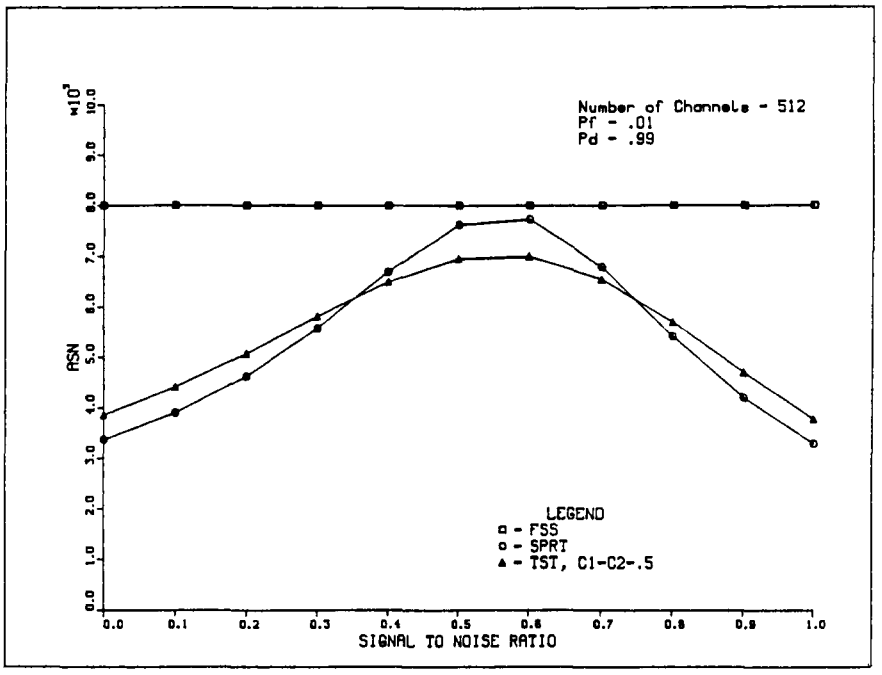

Figure 3: ASN from Theory versus S/N, $\gamma = 1$

assumed signal-to-noise ratio $\gamma = 1$ while Figure 4 and Figure 5 are the corresponding curves for ($\gamma = 0.3$). As promised, the ASN is greatly reduced, by about 57%, for the SPRT in the regions around $\gamma' = 0$ and $\gamma' = \gamma$. These curves exemplify a general property of the SPRT. That is, the SPRT performs very well when the observations statistics are close to those assumed, but the SPRT exhibits a degraded performance, often to the point of being worse than the FSS test, when the observations statistics are different. In our context, this degradation is evidenced by a large ASN for the SPRT when the actual signal-to-noise γ' is midway between the two assumed values 0 and γ. The TST reduces the ASN's poor performance in this "no man's land" as shown by the figures but it does this at the expense of performance in the regions around $\gamma' = 0$ and $\gamma' = \gamma$. Despite this preformance loss, truncation is necessary for implementation reasons. Plus, it will be shown that the TST has the desirable property of being more sensitive than the SPRT at small signal-to-noise ratio's and that through optimization of the mixture constants, the TST can regain much of what

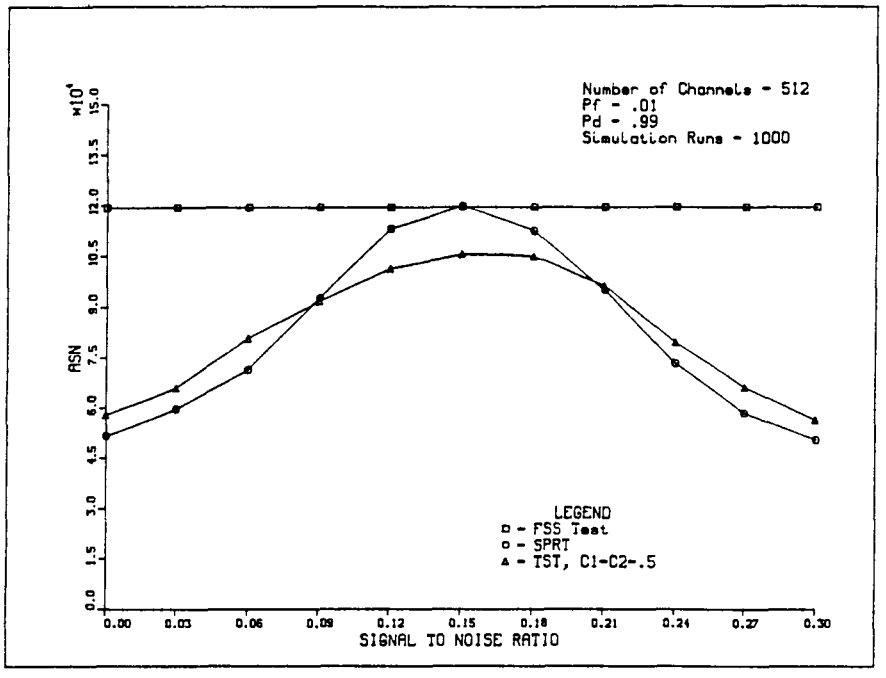

Figure 4: ASN from Simulation versus S/N, $\gamma = 0.3$

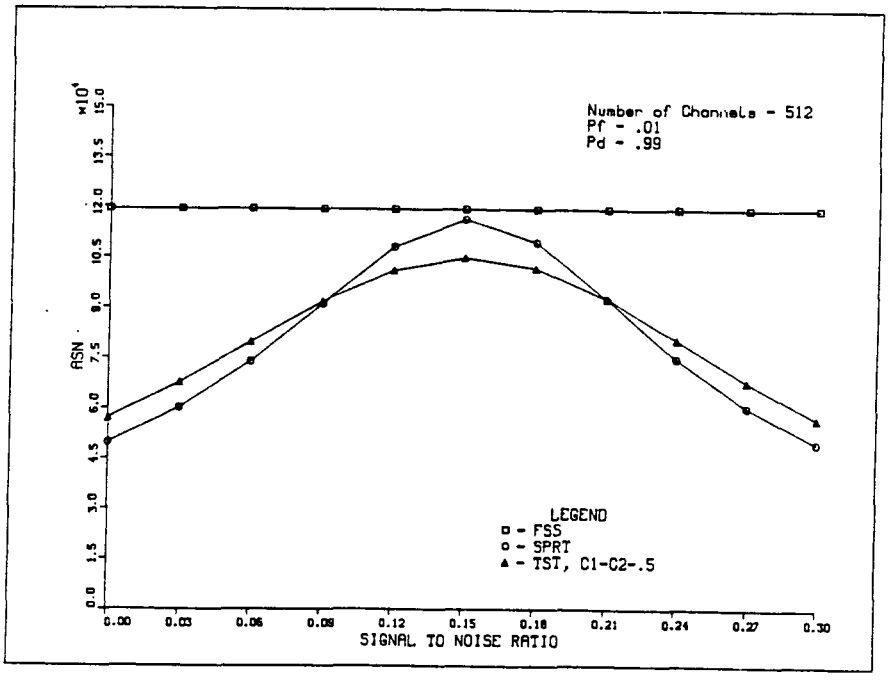

Figure 5: ASN from Theory versus S/N, $\gamma = 0.3$

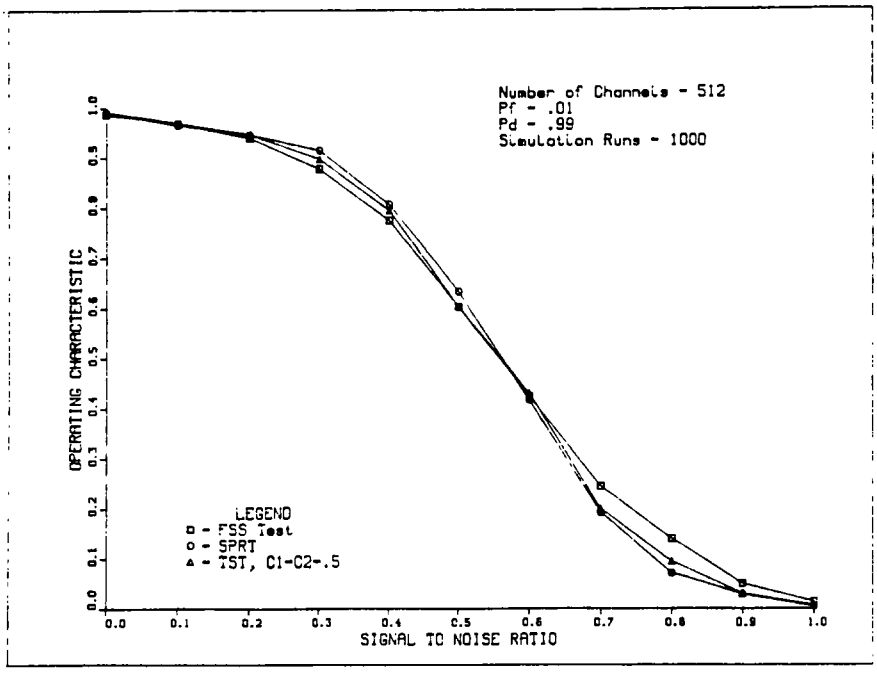

Figure 6: OC from Simulation, $\gamma = 1$

it lost in ASN around $\gamma' = 0$ and $\gamma' = \gamma$.

Focusing on the OCs (Figures 6 and 7 for $\gamma = 1$, Figures 8 and 9 for $\gamma = 0.3$), it is obvious that FSS test is slightly more sensitive for small signal-to-noise ratios while the SPRT has degraded performance in this region. Notice, these test performances are reversed for signal-to-noise ratios close to γ. The OCs also show that the TST's actual detection errors P_F and $1 - P_D$ are within 79% of their bounds use in the TST specification.

Throughout the analysis, various simplifying approximations were made whose accuracies were hard to quantify, especially the Wiener process approximations to the ALLF. Thus, the computer simulation was compared quantitatively to results predicted by theory as a validation of assumptions made. Table 1 for $\gamma = 1$ and Table 2 for $\gamma = 0.3$ show how well the simulation of the three tests correspond to the analysis. The quantity ΔASN is the normalized difference between the theoretical ASN and the simulation ASN where the normalizing factor is the estimated standard

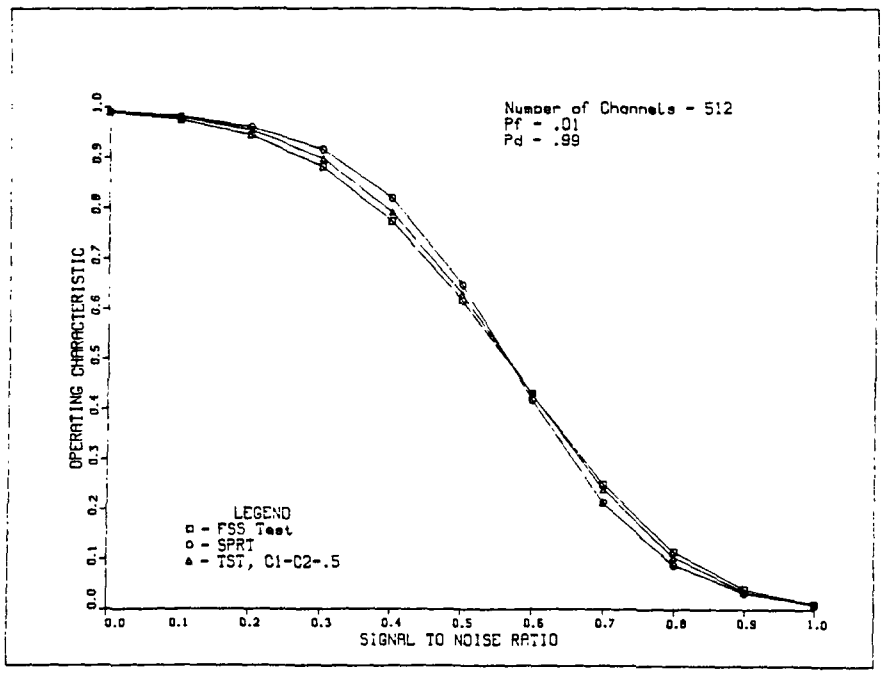

Figure 7: OC from Theory, $\gamma = 1$

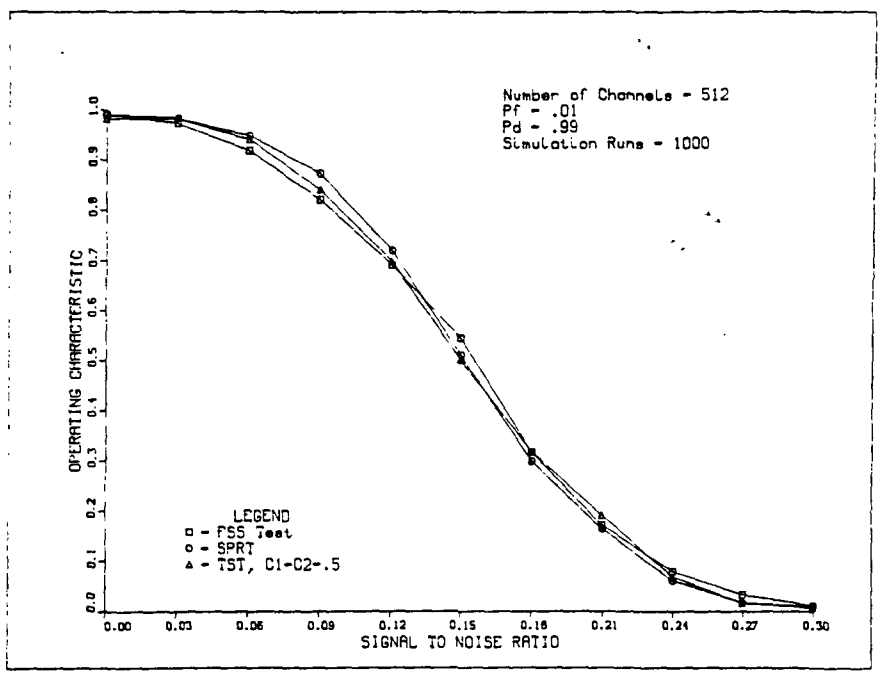

Figure 8: OC from Simulation, $\gamma = 0.3$

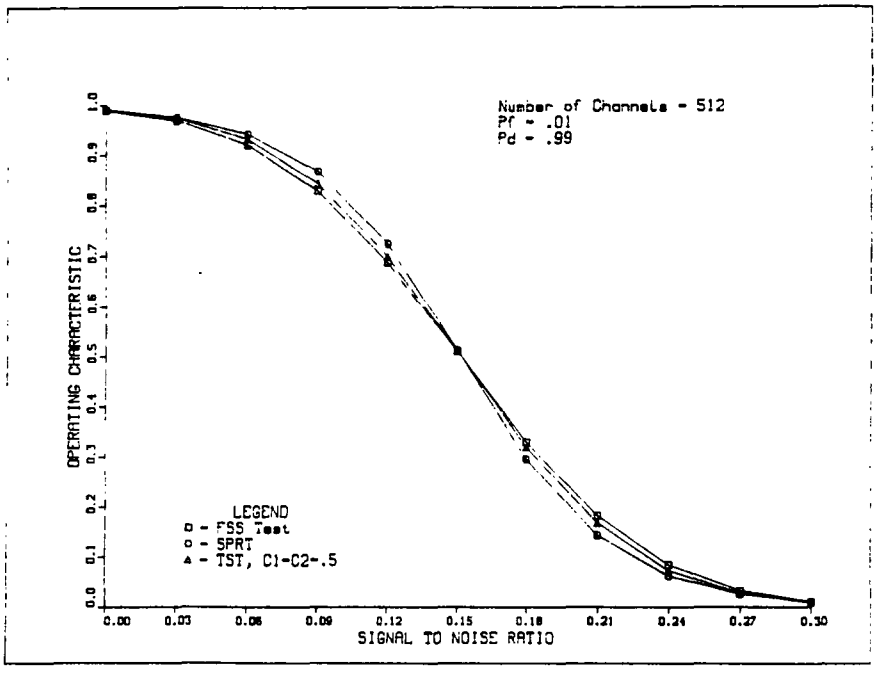

Figure 9: OC from Theory, $\gamma = 0.3$

Table 1: Comparison Between Theory and Simulation for γ=1

γ'	FSS test		SPRT		TST	
	Δ ASN	Δ OC	Δ ASN	Δ OC	Δ ASN	Δ OC
0.00	0.00	0.84	-1.19	-0.03	-1.47	0.03
0.10	0.00	1.11	-0.48	2.77	-0.76	2.03
0.20	0.00	0.45	-1.05	1.92	-1.84	1.02
0.30	0.00	0.18	1.16	-0.09	1.19	-0.18
0.40	0.00	-0.25	1.09	0.89	0.20	-0.40
0.50	0.00	0.73	0.60	0.83	-0.64	1.53
0.60	0.00	0.22	0.23	0.02	-0.14	-0.15
0.70	0.00	0.37	-1.47	1.64	-2.35	3.20
0.80	0.00	-2.16	-0.94	2.25	0.76	1.17
0.90	0.00	-1.33	-1.38	0.83	-1.88	1.02
1.00	0.00	-0.84	-1.16	3.50	-1.38	1.29

Table 2: Comparison Between Theory and Simulation for γ=0.3

γ'	FSS test		SPRT		TST	
	Δ ASN	Δ OC	Δ ASN	Δ OC	Δ ASN	Δ OC
0.00	0.00	-0.71	-1.92	0.02	-1.04	2.09
0.03	0.00	-0.73	0.32	-1.75	1.38	-2.18
0.06	0.00	0.34	1.59	-0.82	-0.71	-1.03
0.09	0.00	0.68	-0.65	-0.49	0.07	0.28
0.12	0.00	-0.24	-1.72	0.33	-0.14	0.08
0.15	0.00	-2.17	-1.09	0.17	-0.48	0.69
0.18	0.00	0.91	-0.96	-0.19	-2.32	0.16
0.21	0.00	0.88	-1.04	-1.83	-2.49	-1.93
0.24	0.00	0.56	0.98	0.09	0.78	0.43
0.27	0.00	-0.18	1.79	2.02	1.70	2.68
0.30	0.00	-0.30	-0.70	1.67	0.63	0.20

deviation of the average used to estimate the ASN. The ΔASN values show a good correspondence between theory and simulation since they are within two standard deviations 86% of the time. The quantity ΔOC is the normalized difference between the theoretical OC and the simulation OC. Here, the normalizing factor is the standard deviation of OC average assuming theoretical OC value is correct. In other words, the normalizing factor for a theoretical OC of $P_0(\gamma')$ and 1000 simulation runs is $\sigma_{OC} = \sqrt{P_0(\gamma')[1 - P_0(\gamma')]/1000}$. Here again, a good correspondence between theory and simulation is apparent.

The purpose of the computer simulation was to validate the assumptions made in the specification and analysis of the three tests, the FSS test, SPRT, and TST. The accuracy in which the analysis predicts quantities measured by simulation, as shown above, lends credence to the assumptions made.

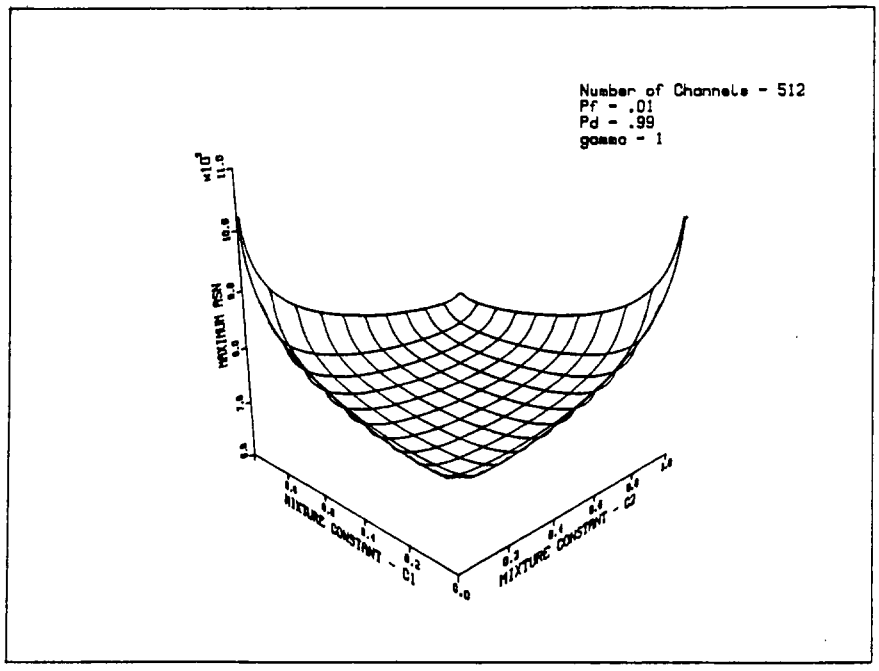

Figure 10: Maximum ASN versus Test Mixture Constants, C_1 and C_2

6 Optimal TST

The analytical expressions; (81) for the ASN and (85) OC of the TST, can be used to determine an TST with an optimum mixture of FSS and SPRT parts. Specifically, the maximum ASN with respect to the signal-to-noise ratio γ varies as a function of the mixture constants C_1 and C_2. This function is graphed in Figure 10. The figure indicates that the optimal TST should have a greater mix of SPRT than that of one half used previously since the maximum ASN of smallest value occurs for smaller values of the mixture constants, C_1 and C_2. This minimum was found numerically and corresponds to mixture constant values of $C_1 = 0.286$ and $C_2 = 0.284$. The ASN and OC of the optimal TST are shown in Figures 11–12. It is interesting that by minimizing the maximum ASN, the ASN in the extreme regions about $\gamma' = 0$ and $\gamma' = \gamma$ are also reduced. This is believed to be a consequence of the optimal TST having a greater SPRT mix than the half-and-half arbitrarily picked before and, therefore, exhibits properties closer to a pure SPRT . Of course, if the first TST

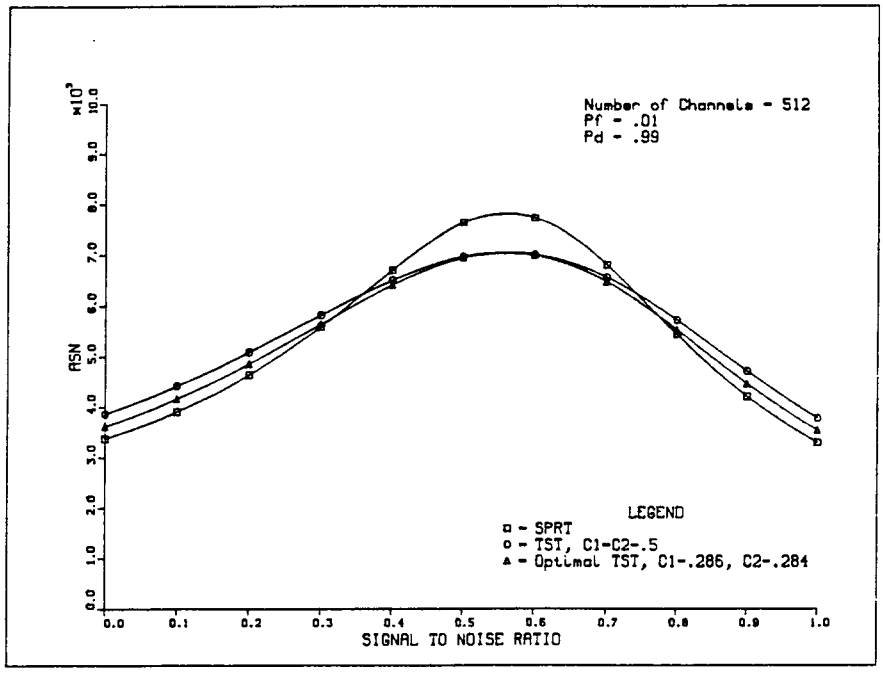

Figure 11: ASN of Optimal TST versus SPRT and TST with $C_1 = 0.5$ and $C_2 = 0.5$

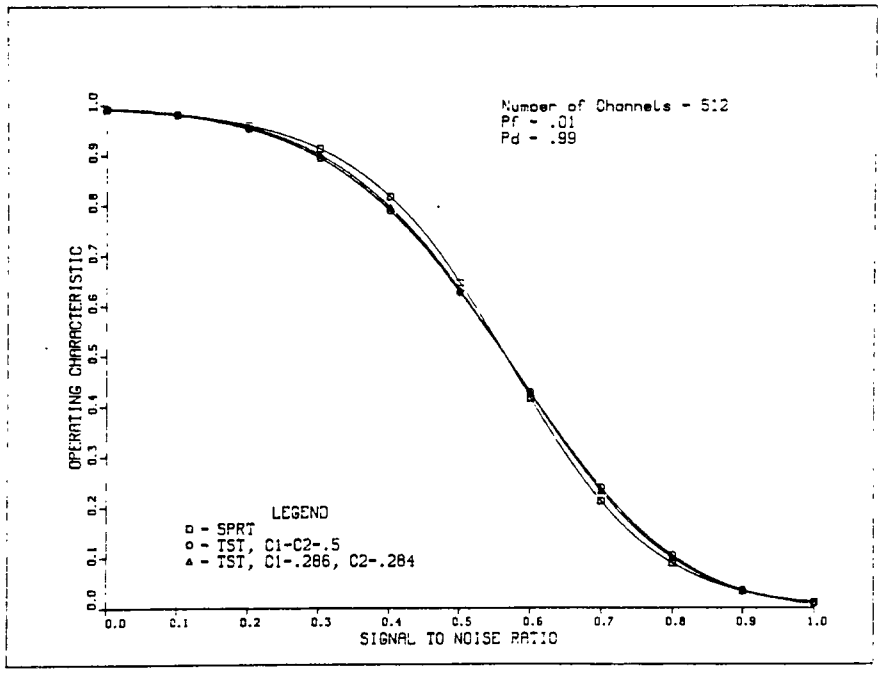

Figure 12: OC of Optimal TST versus SPRT and TST with $C_1 = 0.286$ and $C_2 = 0.284$

was specified to be a primarily SPRT mix, then optimization would have increased the ASN in the extreme regions. The optimal TST offers a good compromise between the need to maximize the ASN performance about the extreme regions and the need to minimize the maximum ASN.

7 Asymptotic Efficiencies

The previous analysis failed to evaluate the performance of the tests when the assumed signal-to-noise ratio γ is small. This case will be examined here. Since the ASN and OC are functions of both γ and the actual signal-to-noise ratio γ', the ASN and OC can be recast as functions of γ and the relative signal-to-noise ratio $r = \sqrt{\gamma'/\gamma}$. In this section, the ASN and OC are defined as functions of γ and r, and will be written as $E(N/r, \gamma)$ and $P_0(r, \gamma)$, respectively. Test performance in the dwindling signal-to-noise ratio case is captured by the limit of the ASN and OC as γ diminishes while r is held constant. For the OC, this is a finite limit, but the ASN limit balloons. Thus, rather than compare the ASNs directly, the limit of the ASN times γ^2 is computed. In other words, a quantity, identified as the asymptotic ASN, $\tilde{E}(N/r)$, will be defined as

$$\tilde{E}(N/r) = \lim_{\gamma \to 0} \gamma^2 E(N/r, \gamma) \tag{86}$$

The asymptotic ASN is useful because it preserves the relative efficiencies between the ASN's as γ diminishes. For instance, consider the FSS test ASN, $E^{FSS}(N/r, \gamma)$, and the SPRT ASN, $E^{SPRT}(N/r, \gamma)$, then

$$\lim_{\gamma \to 0} \frac{E^{FSS}(N/r, \gamma)}{E^{SPRT}(N/r, \gamma)} = \frac{\tilde{E}^{FSS}(N/r)}{\tilde{E}^{SPRT}(N/r)} \tag{87}$$

where $\tilde{E}^{FSS}(N/r)$ are $\tilde{E}^{SPRT}(N/r)$ are the asymptotic ASNs of the FSS test and SPRT, respectively. The asymptotic OC is simply defined as

$$\tilde{P}_0(r) = \lim_{\gamma \to 0} P_0(r, \gamma) \tag{88}$$

As an aid in evaluating these limits, we have asymptotic expressions for moments of the single-epoch ALLF derived in Appendix B are defined as follows

$$\mathcal{M}_r = \tilde{\mathcal{M}}_r \gamma^2 + \mathcal{O}(\gamma^3) \tag{89}$$

$$\mathcal{V}_r = \tilde{\mathcal{V}}_r \gamma^2 + \mathcal{O}(\gamma^3) \tag{90}$$

where

$$\tilde{\mathcal{M}}_r = \frac{K+2}{K^2}(r - \frac{1}{2}) \tag{91}$$

$$\tilde{\mathcal{V}}_r = \frac{K+2}{K^2} \tag{92}$$

Here and throughout this discussion, the quantity $\mathcal{O}(\gamma^n)$ represents any function, say $f(\gamma)$, such that

$$\gamma^{-n} \lim_{\gamma \to 0} f(\gamma) < \infty \tag{93}$$

The particular function represented by $\mathcal{O}(\gamma^n)$ is determined from the context of the equation in which it appears.

To ease the expression of the asymptotic ASN and asymptotic OC, the variables, $\tilde{L}$, $\tilde{\tau}$, $\tilde{a}$, and $\tilde{b}$ are defined. They will be labeled the asymptotic test parameters. Depending on the test type, they have expressions that correspond to that test type's parameter equations where $\mathcal{M}_r$ is replaced with $\tilde{\mathcal{M}}_r$ and likewise $\mathcal{V}_r$ is replaced with $\tilde{\mathcal{V}}_r$. For instance, the FSS asymptotic test parameters are from (60) and (61)

$$\tilde{L} = \frac{\left[\tilde{\mathcal{V}}_1^{\frac{1}{2}} \Phi^{-1}(1 - P_D) - \tilde{\mathcal{V}}_0^{\frac{1}{2}} \Phi^{-1}(1 - P_F)\right]^2}{\left(\tilde{\mathcal{M}}_1 - \tilde{\mathcal{M}}_0\right)^2} \tag{94}$$

$$\tilde{\tau} = \frac{\tilde{L}^{\frac{1}{2}}}{(\tilde{\mathcal{M}}_1 - \tilde{\mathcal{M}}_0)} \left[\tilde{\mathcal{V}}_0^{\frac{1}{2}} \tilde{\mathcal{M}}_1 \Phi^{-1}(1 - P_F) - \tilde{\mathcal{V}}_1^{\frac{1}{2}} \tilde{\mathcal{M}}_0 \Phi^{-1}(1 - P_D)\right] \tag{95}$$

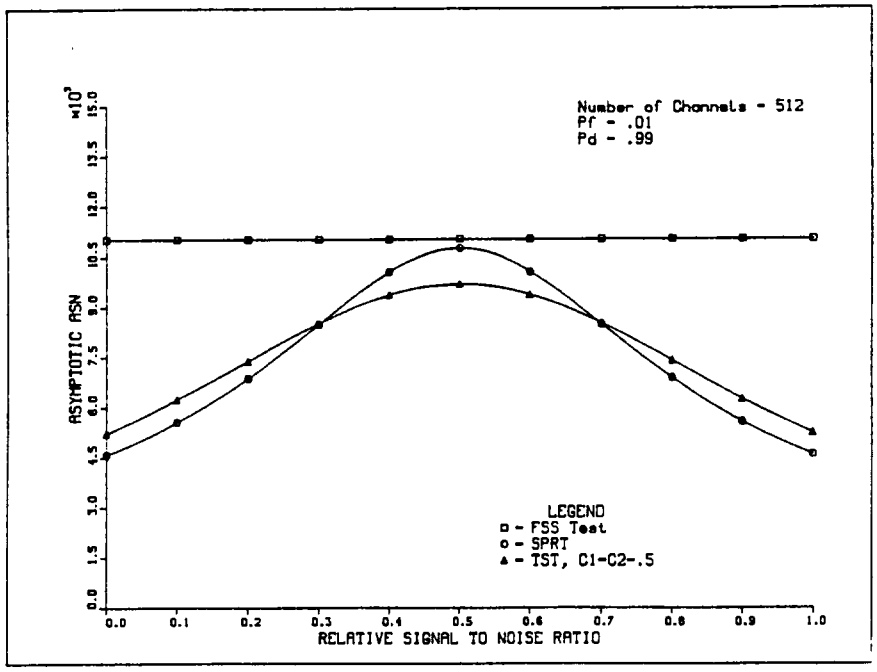

Figure 13: Asymptotic ASN of FSS Test, SPRT, and TST

By using the asymptotic expressions (89) and (90), we have proved that the asymptotic ASN and OC of a test are exactly the ASN and OC of a test with the corresponding asymptotic test parameters. For example, this fact implies from (78) that for the FSS test the asymptotic ASN is

$$\tilde{E}^{FSS}(N/r) = \tilde{L} \tag{96}$$

while the FSS test's asymptotic OC is

$$\tilde{P}_0(r) = \Phi\left(\frac{\tilde{\tau} - \tilde{L}\tilde{\mathcal{M}}_r}{\sqrt{\tilde{L}\tilde{\mathcal{V}}_r}}\right) \tag{97}$$

The ASN and OC for the three different tests were plotted and are compared in Figures 13 and 14. The relative relationship between the test's asymptotic ASNs is almost exactly like that between the ASN's for $\gamma = 1$ and $\gamma = 0.3$ shown in Figures 2–5. This indicates that the three tests have already reached their asymptotes even for $\gamma = 1$. This comment also applies to the OCs. The usefulness of this asymptotic analysis, beyond verifying that the relative gains between tests

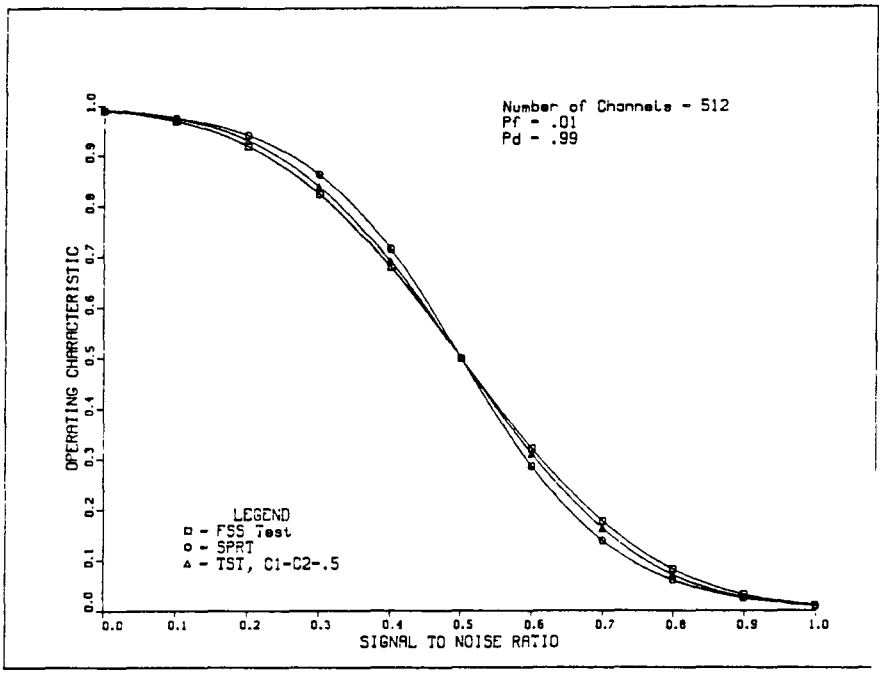

Figure 14: Asymptotic OC Function of FSS Test, SPRT, and TST

remain the same for diminishing signal-to-noise ratio, is that it simplifies the dependence of the test parameters with respect to the parameter γ. Thus for each test, we could choose parameters: $L = \tilde{L}\gamma^{-2}$, $\tau = \tilde{\tau}$, $a = \tilde{a}$, and $b = \tilde{b}$, and have comparable performance for any small γ. This feature simplifies any adaptation with respect to γ that might be added to this detection scheme.

8 Conclusions

Methods for the detection of noncoherent fast FH waveforms have been developed. In the process, the FH waveform was modeled to have an information component which consisted of a series of chips with a known constant epoch where each chip frequency is one of a known ensemble of frequencies. In the model, a particular chip frequency is independently determined by a uniform random variable on the frequency ensemble. The FH waveform was also assumed to have an additive white noise component. By assuming the modeled FH waveform was of a known signal-to-noise

ratio, likelihood-ratio theory spawned the optimal detector based on a single-epoch observation (SELF). SELF was the sum of many nearly identical and nearly independent random variables and thus had nearly Gaussian statistics. This central limit argument allowed a multiepoch collection of SELFs to be considered an equivalent set of Gaussian i.i.d. variables. From these simplified observations, a log-likelihood ratio (ALLF) was computed that was asymptotic to the exact log-likelihood ratio as the number of possible hop frequencies becomes large. ALLF became the test statistic from which three detection tests were based. The tests were: the FSS test, SPRT, and TST. These were defined to ensure that detection errors were below desired levels. By modeling the ALLF as Wiener process, diffusion theory yielded the performance of the three tests not only for a FH waveform of the assumed signal-to-noise but, more generally, the test performance for all signal-to-noise ratios below the one assumed. This analysis compared favorably with a computer simulation of the detector and thus validated the analysis. The analysis also became a tool used to numerically optimize performance of the TST when the actual FH signal-to-noise deviated from that assumed. In order to capture the performance of tests synthesized by assuming an extremely small FH signal-to-noise, expressions for the asymptotic test efficiencies were computed. This asymptotic analysis also yielded simplified test parameter expressions applicable to the small signal-to-noise ratio case.

A significant feature of the SPRT, exposed by the analysis, is that, with the same error probabilities, a frequency-hopped waveform with a known signal-to-noise ratio can be detected in less than half the time of the corresponding fixed sample size test. This reduction in detection time can be used to develop a more sensitive detector which is especially significant for Low Probability of Intercept (LPI) applications where the transmissions are purposely short. For the pure SPRT,

detection time increased whenever the observed signal-to-noise ratio differed from that assumed in the test's synthesis. And in some instances, it was even comparable to the corresponding FSS test. The TST significantly improves this anomaly while sacrificing little performance over that of the purely sequential test. Plus, the optimal TST can regain much of this lost performance while still smoothing out the SPRT anomaly. The decrease in the detection time of the sequential tests can be used to robustify the test with respect to the input signal-to-noise ratio with it still having performance exceeding that of the FSS test. The simplified test parameter expressions derived by asymptotic methods may be useful for any schemes to adapt these tests for FH signal-to-noise ratios.

It is apparent that other simplifications and extensions to these results are possible. For instance, it was assumed that the starting time and duration of the chip epoch were known. This first restriction might be relaxed by redefining the SELF to perform sliding window integration instead of the integrate and dump operation now performed. This, of course, would degrade the detector's performance for some values of epoch starting time, but it would probably exhibit a better average performance. There are also possible simplifications to the SELF to improve it's implementability.

A Derivation of SELF

Proceeding from Appendix B of [1], the likelihood function, given the carrier phase θ and the channel k, the conditional likelihood function for the ith epoch is

$$\Lambda_i(y/k,\theta) = e^{-\frac{E}{N_0}} e^{\frac{2}{N_0}\int_{iT_h}^{(i+1)T_h} y(t)x_i(t)dt} \tag{98}$$

where E is the single-epoch energy of the FH signal, i.e.

$$E = \int_{iT_h}^{(i+1)T_h} 2S\sin^2(\omega_{k_i}t+\theta)dt \tag{99}$$

By applying a half-angle trigonometric identity, the energy integral becomes

$$E = S(T_h + \epsilon) \tag{100}$$

where

$$\epsilon = \int_{iT_h}^{(i+1)T_h} \cos(2\omega_{k_i} t + 2\theta) dt \tag{101}$$

But since

$$|\epsilon| \leq \frac{1}{\omega_{k_i}} \tag{102}$$

we have

$$E \approx ST_h \qquad \text{for } \omega_{k_i} T_h \gg 1 \tag{103}$$

Substituting this approximation for E into the conditional likelihood function (98) and expanding $x_i(t)$ yields

$$\Lambda_i\,(y/k, \theta) = e^{-\gamma} e^{\sqrt{2\gamma}(P_k \sin\theta + Q_k \cos\theta)} \tag{104}$$

where

$$\begin{aligned} P_k &= \frac{2}{\sqrt{N_0 T_h}} \int_{iT_h}^{(i+1)T_h} y(t) \cos\omega_{k_i} t \, dt \\ Q_k &= \frac{2}{\sqrt{N_0 T_h}} \int_{iT_h}^{(i+1)T_h} y(t) \sin\omega_{k_i} t \, dt \end{aligned} \tag{105}$$

Taking Expectations with respect to θ defines

$$\Lambda_i(y/k) \triangleq E_\theta\,[\Lambda_i(y/k, \theta)] \tag{106}$$

which is the likelihood function conditional only on the channel. This expectation can be evaluated as follows

$$E_\theta\,[\Lambda_i(y/k, \theta)] = \frac{e^{-\gamma}}{2\pi} \int_0^{2\pi} e^{\sqrt{2\gamma}(P_k \sin\theta + Q_k \cos\theta)} d\theta \tag{107}$$

$$= \frac{e^{-\gamma}}{2\pi} \int_0^{2\pi} e^{\sqrt{2\gamma}\sqrt{P_k^2 + Q_k^2} \sin(\theta + \psi)} d\theta \tag{108}$$

where $\psi = \text{Arg}(P_k + jQ_k)$. Now by the periodicity of the integrand

$$E_\theta\left[\Lambda_i(y/k,\theta)\right] = \frac{e^{-\gamma}}{2\pi}\int_0^{2\pi} e^{\sqrt{2\gamma}\sqrt{P_k^2+Q_k^2}\cos\theta}d\theta \tag{109}$$

$$= e^{-\gamma} I_0\left(\sqrt{2\gamma}\sqrt{P_k^2+Q_k^2}\right) \tag{110}$$

by the identity

$$I_0(a) = \frac{1}{2\pi}\int_0^{2\pi} e^{a\cos\theta}d\theta \tag{111}$$

where I_0 is the zeroth order modified Bessel function of the first kind. Taking expectations with respect to the channel k yields the Single-Epoch Likelihood Function (SELF)

$$\Lambda_i(y) \triangleq E_k\left[\Lambda_i(y/k)\right] \tag{112}$$

$$= \frac{e^{-\gamma}}{K}\sum_{k=0}^{K-1} I_0\left(\sqrt{2\gamma}\sqrt{P_k^2+Q_k^2}\right) \tag{113}$$

B Asymptotic Expressions of the ALLF Moments

We want to examine the behavior of the ALLF moments when signal-to-noise ratio γ diminishes while the relative signal-to-noise ratio r is held constant. The asymptotic expressions derived here encapsulate this behavior. To derive asymptotic expressions for the mean and variance of the ALLF, we need only consider the mean and variance, $\mathcal{M}_r$ and $\mathcal{V}_r$, of the single-epoch ALLF. To this end, it will be useful to derive asymptotic expression of two functions of the channel moments: μ_r/σ_0 and σ_r^2/σ_0^2. Starting with the first expression and substituting equations (31),

$$\frac{\mu_r^2}{\sigma_0^2} = \frac{I_0^2(2r\gamma)}{[I_0(2\gamma)-1]} \tag{114}$$

We will need a partial power series expansion of $I_0(x)$, i.e.

$$I_0(x) = 1 + \frac{x^2}{4} + \frac{x^4}{64} + \mathcal{O}(x^6) \tag{115}$$

Here and throughout this discussion, the quantity $\mathcal{O}(x^n)$ represents any function, say $f(x)$, such that

$$x^{-n} \lim_{x \to 0} f(x) < \infty \tag{116}$$

The particular function represented by $\mathcal{O}(x^n)$ is determined from the context of the equation in which it appears. With the above power series for I_0, (114) becomes

$$\frac{\mu_r^2}{\sigma_0^2} = \frac{\left[1 + r\gamma^2 + \mathcal{O}(\gamma^4)\right]^2}{\gamma^2 + \frac{1}{4}\gamma^4 + \mathcal{O}(\gamma^6)} \tag{117}$$

$$= \frac{1 + 2r\gamma^2 + \mathcal{O}(\gamma^4)}{\gamma^2 + \frac{1}{4}\gamma^4 + \mathcal{O}(\gamma^6)} \tag{118}$$

$$= \gamma^{-2} + \left(2r - \tfrac{1}{4}\right) + \mathcal{O}(\gamma^2) \tag{119}$$

$$= \left[\gamma^{-1} + \left(r - \tfrac{1}{8}\right)\gamma + \mathcal{O}(\gamma^3)\right]^2 \tag{120}$$

thus

$$\frac{\mu_r}{\sigma_0} = \gamma^{-1} + \left(r - \tfrac{1}{8}\right)\gamma + \mathcal{O}(\gamma^3) \tag{121}$$

Now to evaluate the second channel moment function. Using equations (31) and (115), plus the power series for e^x, we get after carrying out the multiplications

$$\frac{\sigma_r^2}{\sigma_0^2} = [I_0(2\gamma) - 1]^{-1} \left[\frac{1}{\pi}\int_0^\pi e^{-2\gamma\cos\phi} I_0(4r\gamma \sin\frac{\phi}{2}) d\phi - I_0^2(2r\gamma)\right] \tag{122}$$

$$\begin{aligned}\frac{\sigma_r^2}{\sigma_0^2} = \left[\gamma^2 + \tfrac{1}{4}\gamma^4 + \mathcal{O}(\gamma^6)\right]^{-1} \Bigg\{ & \frac{1}{\pi}\int_0^\pi \\ & \left[1 - 2\gamma\cos\phi + 2\gamma^2\cos^2\phi - \tfrac{4}{3}\gamma\cos^3\phi^3 + \tfrac{2}{3}\cos^4\phi\gamma^4 + \mathcal{O}(\gamma^5)\right] \times \\ & \left[1 + 4r\gamma^2\sin^2\tfrac{\phi}{2} + 4r^2\gamma^4\sin^4\tfrac{\phi}{2} + \mathcal{O}(\gamma^6)\right] d\phi \\ & - \left[1 + r\gamma^2 + \tfrac{1}{4}r^2\gamma^4 + \mathcal{O}(\gamma^6)\right]^2 \Bigg\}\end{aligned} \tag{123}$$

$$\begin{aligned}\frac{\sigma_r^2}{\sigma_0^2} &= \left[\gamma^2 + \tfrac{1}{4}\gamma^4 + \mathcal{O}(\gamma^6)\right]^{-1} \left\{ \frac{1}{\pi}\int_0^\pi \left[1 - 2\cos\phi\,\gamma \right.\right. \\ &+ \left(4r\sin^2\tfrac{\phi}{2} + 2\cos^2\phi\right)\gamma^2 - \left(8r\cos\phi\sin^2\tfrac{\phi}{2} + \tfrac{4}{3}\cos^3\phi\right)\gamma^3 \\ &\left.\left. + \left(\tfrac{2}{3}\cos^4\phi + 8r\cos^2\phi\sin^2\tfrac{\phi}{2} + 4r^2\sin^4\tfrac{\phi}{2}\right)\gamma^4 + \mathcal{O}(\phi,\gamma^5)\right] d\phi \right. \\ &\left. - \left[1 + 2r\gamma^2 + \tfrac{3}{2}r^2\gamma^4 + \mathcal{O}(\gamma^6)\right] \right\}\end{aligned} \tag{124}$$

Let $f(\phi,\gamma^5)$ be the particular function represented by the symbol $\mathcal{O}(\phi,\gamma^5)$ under the integral then

$$\lim_{\gamma\to 0}\gamma^{-5}\int_0^\pi f(\phi,\gamma^5) = \int_0^\pi \lim_{\gamma\to 0}\gamma^{-5} f(\phi,\gamma^5) < \infty \tag{125}$$

implying that $\int_0^\pi f(\phi,\gamma^5) \in \mathcal{O}(\gamma^5)$. The interchange of the limit and integration is justified as follows. The function $f(\phi,\gamma^5)$ inherents continuity on the compact set $\{\phi,\gamma : \phi \in [0,\pi]$ and $\gamma \in [0,1]\}$ from the integrand of which it is a component. Therefore $\gamma^{-5}f(\phi,\gamma^5)$, which is has a finite limit at the origin, is also continuous on this compact set and hence is bounded, say by B, on this set. The function B is integrable on $\phi \in [0,\pi]$ by which the interchange follows by the Lebesgue Dominated Convergence theorem. The interchange implies that (124) can be integrated term-wise to yield

$$\begin{aligned}\frac{\sigma_r^2}{\sigma_0^2} &= \left[\gamma^2 + \tfrac{1}{4}\gamma^4 + \mathcal{O}(\gamma^6)\right]^{-1} \times \\ &\left\{\left[1 + (2r+1)\gamma^2 + 2r^2\gamma^3 + (\tfrac{1}{4} + 2r + \tfrac{3}{2}r^2)\gamma^4 + \mathcal{O}(\gamma^5)\right]\right. \\ &\left. - \left[1 + 2r\gamma^2 + \tfrac{3}{2}r^2\gamma^4 + \mathcal{O}(\gamma^6)\right]\right\}\end{aligned} \tag{126}$$

which simplifies to

$$\frac{\sigma_r^2}{\sigma_0^2} = 1 + 2r\gamma + 2r\gamma^2 + \mathcal{O}(\gamma^3) \tag{127}$$

With these asymptotic expressions for μ_r/σ_0 and σ_r^2/σ_0^2, we proceed with the derivation of asymptotic expressions for the ALLF moments. The ALLF mean is expressed in terms of the SELF

moments as

$$\mathcal{M}_r = \frac{1}{2}\ln\frac{V_0}{V_1} + [2V_1V_0]^{-1}\left\{[M_r - M_0]^2 V_1 + [M_r - M_1]^2 V_0 + [V_1 - V_0]V_r\right\} \tag{128}$$

The last three terms can be evaluated as follows

$$\begin{aligned}
&[2V_1V_0]^{-1}\left\{[M_r - M_0]^2 V_1 + [M_r - M_1]^2 V_0 + [V_1 - V_0]V_r\right\} \\
&= \frac{1}{2K}\left[K - 1 + \frac{\sigma_1^2}{\sigma_0^2}\right]^{-1}\left\{\left[\frac{\mu_r}{\sigma_0} - \frac{\mu_0}{\sigma_0}\right]^2\left[K - 1 + \frac{\sigma_1^2}{\sigma_0^2}\right]\right. \\
&\quad \left. -K\left[\frac{\mu_0}{\sigma_0} - \frac{\mu_1}{\sigma_0}\right]^2 + \left[K - 1 + \frac{\sigma_r^2}{\sigma_0^2}\right]\left[\frac{\sigma_1^2}{\sigma_0^2} - 1\right]\right\} \qquad (129) \\
&= \frac{1}{2K}\left[K + 2\gamma + \mathcal{O}(\gamma^2)\right]^{-1}\left\{[r\gamma + \mathcal{O}(\gamma^3)]^2[K + \mathcal{O}(\gamma)]\right. \\
&\quad -K\left[(r-1)\gamma + \mathcal{O}(\gamma^3)\right]^2 \times \\
&\quad \left.[K + 2r\gamma + \mathcal{O}(\gamma^2)]\left[2\gamma + 2\gamma^2 + \mathcal{O}(\gamma^3)\right]\right\} \qquad (130) \\
&= \frac{\gamma}{K} + \left(\frac{K+2}{K^2}r + \frac{K-4}{2K^2}\right)\gamma^2 + \mathcal{O}(\gamma^3) \qquad (131)
\end{aligned}$$

Now for the final term. We will need the the following power series expansion for $\ln(x)$

$$\ln(1+x) = x - \frac{x^2}{2} + \mathcal{O}(x^3) \tag{132}$$

$$\begin{aligned}
\frac{1}{2}\ln\left(\frac{V_0}{V_1}\right) &= -\frac{1}{2}\ln\left[1 - \frac{1}{K} + \frac{1}{K}\frac{\sigma_1^2}{\sigma_0^2}\right] &(133)\\
&= -\frac{1}{2}\ln\left[1 + \frac{2}{K}\gamma + \frac{2}{K}\gamma^2 + \mathcal{O}(\gamma^3)\right] &(134)\\
&= -\frac{\gamma}{K} + \left(\frac{1}{K^2} - \frac{1}{K}\right)\gamma^2 + \mathcal{O}(\gamma^3) &(135)
\end{aligned}$$

combining (131) and (135)

$$\mathcal{M}_r = \frac{K+2}{K^2}\left(r - \frac{1}{2}\right)\gamma^2 + \mathcal{O}(\gamma^3) \tag{136}$$

Now to proceed with the variance.

$$\mathcal{V}_r = \frac{V_r^2}{2}\left(\frac{1}{V_0} - \frac{1}{V_1}\right)^2 + \left[\left(\frac{1}{V_0} - \frac{1}{V_1}\right)M_r + \left(\frac{M_1}{V_1} - \frac{M_0}{V_0}\right)\right]^2 V_r \tag{137}$$

The first term can be evaluated as

$$\frac{V_r^2}{2}\left(\frac{1}{V_0} - \frac{1}{V_1}\right)^2 = \frac{1}{2K^2}\left\{\frac{\left[\frac{\sigma_1^2}{\sigma_0^2} - 1\right]\left[K - 1 + \frac{\sigma_r^2}{\sigma_0^2}\right]}{\left[K - 1 + \frac{\sigma_1^2}{\sigma_0^2}\right]}\right\}^2 \tag{138}$$

$$= \frac{1}{2K^2}\left\{\frac{[2\gamma + \mathcal{O}(\gamma^2)]\,[K + \mathcal{O}(\gamma)]}{[K + \mathcal{O}(\gamma)]}\right\}^2 \tag{139}$$

$$= \frac{2\gamma^2}{K^2} + \mathcal{O}(\gamma^3) \tag{140}$$

The second term of (137)

$$\left[\left(\frac{1}{V_0} - \frac{1}{V_1}\right)M_r + \left(\frac{M_1}{V_1} - \frac{M_0}{V_0}\right)\right]^2 V_r$$

$$= \frac{1}{K^2}\frac{\left[K - 1 + \frac{\sigma_r^2}{\sigma_0^2}\right]}{\left[K - 1 + \frac{\sigma_1^2}{\sigma_0^2}\right]^2}\left\{\left[\frac{\sigma_1^2}{\sigma_0^2} - 1\right]\left[(K-1)\frac{\mu_0}{\sigma_0} + \frac{\mu_r}{\sigma_0}\right] + K\left[\frac{\mu_1}{\sigma_0} - \frac{\mu_0}{\sigma_0}\frac{\sigma_1^2}{\sigma_0^2}\right]\right\}^2 \tag{141}$$

$$= \frac{1}{K^2}\frac{[K + \mathcal{O}(\gamma)]}{[K + \mathcal{O}(\gamma)]^2}\left\{\begin{array}{l}\left[2\gamma + 2\gamma^2 + \mathcal{O}(\gamma^3)\right]\left[K\gamma^{-1} + \mathcal{O}(\gamma)\right] \\ \quad + K\left[\gamma^{-1} + \frac{7}{8}\gamma + \mathcal{O}(\gamma^3)\right] \\ \quad - K\left[\gamma^{-1} - \frac{1}{8}\gamma + \mathcal{O}(\gamma^3)\right]\left[1 + 2\gamma + 2\gamma^2 + \mathcal{O}(\gamma^3)\right]\end{array}\right\}^2 \tag{142}$$

$$= \frac{1}{K^2} \frac{[K + \mathcal{O}(\gamma)]}{[K + \mathcal{O}(\gamma)]^2} \left\{ [2K + 2K\gamma + \mathcal{O}(\gamma^2)] + K [-2 - \gamma + \mathcal{O}(\gamma^2)] \right\}^2 \quad (143)$$

$$= \frac{\gamma^2}{K} + \mathcal{O}(\gamma^3) \quad (144)$$

Combining (140) and (144) yields

$$\mathcal{V}_r = \frac{K+2}{K^2}\gamma^2 + \mathcal{O}(\gamma^3) \quad (145)$$

Summarizing these results

$$\mathcal{M}_r = \frac{K+2}{K^2}\left(r - \frac{1}{2}\right)\gamma^2 + \mathcal{O}(\gamma^3) \quad (146)$$

$$\mathcal{V}_r = \frac{K+2}{K^2}\gamma^2 + \mathcal{O}(\gamma^3) \quad (147)$$

References

[1] D.G. Woodring, "Performance of Optimum and Suboptimum Detectors for Spread Spectrum Waveforms", Naval Research Laboratory, Washington, DC, Technical Report No. 8432, December 1980.

[2] J.D. Edell, "Wideband, noncoherent, frequency-hopped waveforms and their hybrids in low-probability-of-intercept communications", Naval Research Laboratory, Washington, DC, Technical Report No. 8025, November 1976.

[3] A. Wald, *Sequential Analysis*, Wiley, New York, 1947.

[4] N. Shiryayev, *Optimal Stopping Rules*, Springer-Verlag, New York, 1977.

[5] D.A. Darling and A.J.F. Siegert, "The first passage problem for a continuous Markov process", *Ann. Math. Stat.*, vol. 24, pp. 624–639, 1953.

[6] T.W. Anderson, "A modification of the sequential probability ratio test to reduce the sample size", *Ann. Math. Stat.*, vol. 31, pp. 165–197, 1960.

[7] S. Tantaratana and H.V. Poor, "Asymptotic efficiencies of truncated sequential tests", *IEEE Trans. Inform. Theory*, vol. IT-28, no. 6, pp. 911–923, November 1982.

[8] S. Tantaratana and J.B. Thomas, "Truncated sequential probability ratio test", *Inform. Sci.*, vol. 13, pp. 283–300, 1977.

[9] C.B. Read, "The partial sequential probability ratio tests", *J Amer. Statist. Assoc.*, vol. 66, pp. 646–650, 1971.

[10] G.N. Watson, *A Treatise on the Theory of Bessel Functions*, Cambridge University Press, New York, 1980.